

Heterobimetallic alkoxysilyl cationic complexes: investigations into the displacement of a $\mu\text{-}\eta^2\text{-Si,O}$ bridge by functional phosphine ligands

Joël Blin,^a Pierre Braunstein,^a Jean Fischer,^b Guido Kickelbick,^c Michael Knorr,^a Xavier Morise^a and Tobias Wirth^a

^a Laboratoire de Chimie de Coordination (UMR 7513 CNRS), Université Louis Pasteur, 4 rue Blaise Pascal, F-67070 Strasbourg Cédex, France

^b Laboratoire de Cristallogénie et de Chimie Structurale (UMR 7513 CNRS), Université Louis Pasteur, 4 rue Blaise Pascal, F-67070 Strasbourg Cédex, France

^c Institut für Anorganische Chemie, Technische Universität Wien, Getreidemarkt 9/1153, A-1060 Wien, Austria

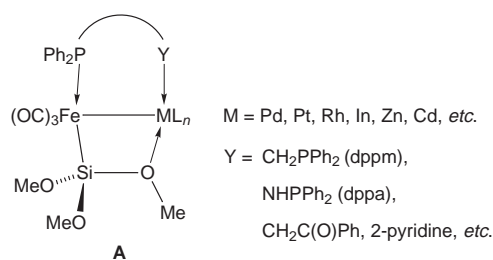
Received 13th January 1999, Accepted 5th May 1999

The lability of the $\text{SiO}\rightarrow\text{M}$ interaction unique to some bimetallic complexes may confer hemilabile properties to the $\text{Si}(\text{OR})_3$ ligand and various bifunctional phosphines P–Z have been used in order to evaluate the possible competition for co-ordination between the bridging $\text{SiO}\rightarrow\text{M}$ interaction and P–Z chelation. Thus, treatment of the heterobimetallic complexes $[(\text{OC})_3\text{Fe}\{\mu\text{-Si}(\text{OMe})_2(\text{OMe})\}(\mu\text{-dppm})\text{MCl}]$ ($\text{M} = \text{Pd}$ **4** or Pt **6**; $\text{dppm} = \text{Ph}_2\text{PCH}_2\text{PPh}_2$) and $[(\text{OC})_3\text{Fe}\{\mu\text{-Si}(\text{OMe})_2(\text{OMe})\}(\mu\text{-dppa})\text{PdCl}]$ **5** ($\text{dppa} = \text{Ph}_2\text{PNHPPH}_2$) with TIPF_6 in the presence of P–Z afforded the corresponding cationic compounds $[(\text{OC})_3\text{Fe}\{\mu\text{-Si}(\text{OMe})_2(\text{OMe})\}(\mu\text{-dppm})\text{M}(\text{P-Z})\text{PF}_6]$ ($\text{M} = \text{Pd}$ **1** or Pt **3**) and $[(\text{OC})_3\text{Fe}\{\mu\text{-Si}(\text{OMe})_2(\text{OMe})\}(\mu\text{-dppa})\text{Pd}(\text{P-Z})\text{PF}_6]$ **2** ($\text{P-Z} = \text{Ph}_2\text{PC}_6\text{H}_4(o\text{-OMe})$, **a** $\text{P}\{\text{C}_6\text{H}_4(o\text{-OMe})\}_3$, **b** $\text{Ph}_2\text{PCH}_2\text{C}(\text{O})\text{Ph}$, **c** $\text{Ph}_2\text{PCH}_2\text{CH}=\text{CH}_2$, **d** $\text{Ph}_2\text{P}(\text{CH}_2)_2\text{CN}$, **e** or $\text{Ph}_2\text{PCH}_2\text{C}(\text{O})\text{NPh}_2$, **f**). These complexes are stabilized by the occurrence of a Fe–Si–O→M four-membered ring and the pre-existent $\text{SiO}\rightarrow\text{M}$ interaction in **4–6** was not displaced by the donor function of the incoming P–Z ligand. Complexes **1b** and **1f** were obtained as mixtures of two isomers, the P–Z ligands acting either as monodentate or as a P,O chelate. In the latter cases formation of five-co-ordinated palladium species is proposed. Displacement of the $\text{SiO}\rightarrow\text{Pd}$ interaction originally present in **4** was observed when the diphosphines $(\text{Ph}_2\text{P})_2\text{NR}$ ($\text{R} = \text{Me}$ or $(\text{CH}_2)_3\text{Si}(\text{OEt})_3$) were used, since the two phosphorus atoms co-ordinate to the Pd. Surprisingly these diphosphine ligands show different co-ordination modes, depending on whether dppa or dppm is used as the assembling ligand. In the former case, chelation to the Pd is observed, which leads to complex $[(\text{OC})_3\{\text{MeO}\}_3\text{Si}\{\text{Fe}(\mu\text{-dppa})\text{Pd}\{\text{Ph}_2\text{PN}(\text{Me})\text{PPh}_2\}\}\text{PF}_6]$ **2g**, whereas in the latter case, oligomeric entities of the type $\{[(\text{OC})_3\{\text{MeO}\}_3\text{Si}\{\text{Fe}(\mu\text{-dppa})\text{Pd}\{\text{Ph}_2\text{PN}(\text{R})\text{PPh}_2\}\}_n\}\text{PF}_6$ **1g, 1h** (n probably equals two) were formed. The molecular structures of $[\text{PdCl}(\text{dppm-}P,P')\{\text{Ph}_2\text{PC}_6\text{H}_4(o\text{-OMe})\}\text{PF}_6]$ **g** and $[\text{Pd}_2\text{Cl}_2(\mu\text{-CO})(\mu\text{-dppm})_2]$ **10**, obtained during this work, have been determined by X-ray diffraction.

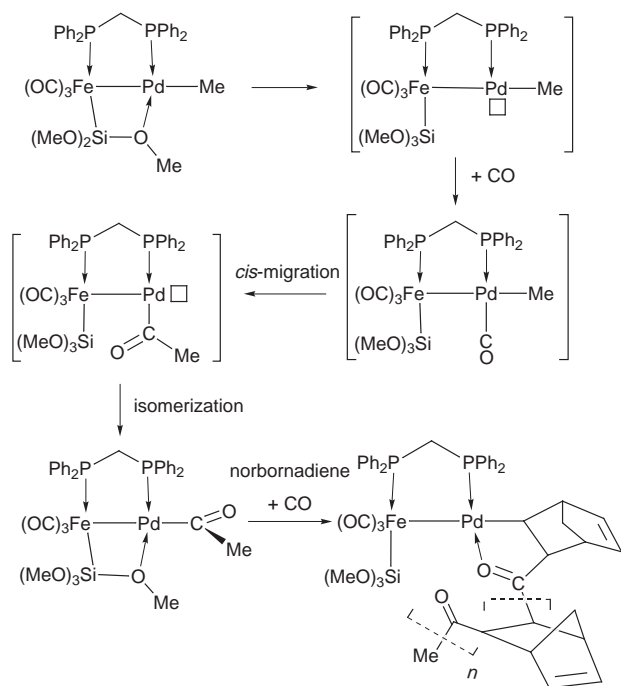
Introduction

During the past decades both complexes containing metal silicon bonds¹ and heteronuclear clusters² have attracted increasing attention owing to their fundamental interest and their catalytic and physico-chemical properties. With the objective of combining the potential of these two classes of compounds, we have investigated the synthesis and the reactivity of heterobimetallic complexes bearing a SiR_3 ligand.^{3a} This led to the discovery that a $\text{Si}(\text{OMe})_3$ unit, which was originally only known as a terminal ligand, could bridge two metal centres.^{3b,c} We have synthesized a series of Fe–M heterobimetallic complexes of type **A** ($\text{M} = \text{Pd}, \text{Pt}, \text{Rh}, \text{In}, \text{Zn}, \text{Cd}, \text{etc.}$), which display a $\mu\text{-}\eta^2\text{-Si,O}$ bridge between the two metal centres. The bifunctional phosphine P–Y acts as an assembling ligand and thus contributes to the stabilization of the entire molecule.⁴

Surprisingly, the dative $\text{O}\rightarrow\text{M}$ interaction is usually not displaced by two-electron donor ligands such as phosphines or amines. However, it is kinetically labile as shown by variable temperature ¹H NMR experiments which revealed the hemilability of the $\text{Si}(\text{OMe})_3$ ligand. The equivalence of the OMe groups above the coalescence temperature results from rapid rotation of the ligand about the Fe–Si axis. This behaviour may



represent an interesting tool for catalytic processes where the storage of a “masked” co-ordination site plays an important role. Indeed we have observed insertion reactions under mild conditions of small molecules such as CO, isocyanides or olefins into the Pd–C or Pt–C bond of such bimetallic complexes.⁵ These reactions proceed *via* the following pattern: opening of the $\text{SiO}\rightarrow\text{Pd}$ interaction, co-ordination of the incoming substrate, *cis* migration, isomerization and closing of the Fe–Si–O→Pd ring. This is depicted in Scheme 1 in the case of CO insertion into a Pd–Me bond, followed by olefin insertion into the resulting palladium–acyl bond. Repetition of these successive steps results in sequential insertion of CO and olefins



Scheme 1

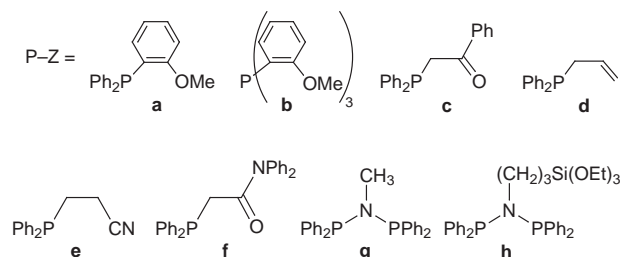
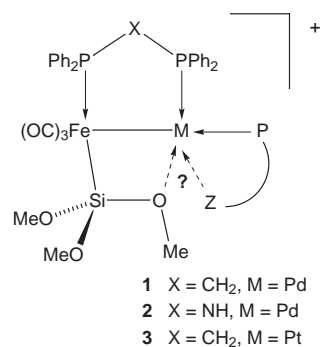
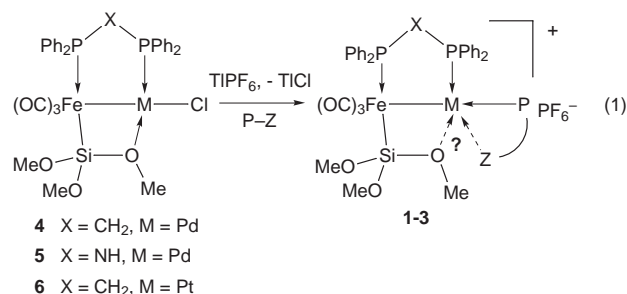
leading to polyketone formation.^{3a,5a} A related mechanism has also been proposed for the dehydrogenative coupling of stannanes catalysed by Fe–Pd complexes.⁶

The above observations prompted us to study the behaviour of the SiO→Pd interaction in the presence of various donor ligands which may compete with it. Infrared monitoring of the reactions in Scheme 1 has evidenced the formation of intermediates in which the oxygen atom of the ketone function of the growing chain co-ordinates to the palladium centre and generates a new Pd–C–C–O five membered ring.^{5a} Thus we found it of interest to investigate whether similar displacements occur when ligands containing ketone or olefin functionalities, such as phosphines Ph₂PCH₂C(O)Ph **c** and Ph₂PCH₂CH=CH₂ **d** respectively, are present in the palladium co-ordination sphere. More generally we were interested in introducing in the co-ordination sphere of the metal M (Pd or Pt) nucleophilic functionalities Z which could potentially form a P,Z chelate, with retention or displacement of the SiO→Pd interaction. It was hoped that such studies could provide useful information about the chelate-assisted co-ordination of unsaturated functional groups which could also mimic the behaviour of substrates during catalytic cycles.

We report here investigations on the synthesis and characterization of a series of cationic heterobimetallic Fe–Pd and Fe–Pt complexes **1–3** containing the closely related assembling ligands dppm and dppa (dppm = Ph₂PCH₂PPh₂; dppa = Ph₂PNHPPH₂) and the functional phosphines P–Z shown below.

Results and discussion

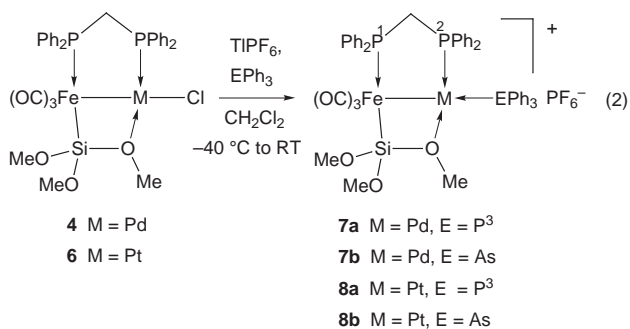
The approach used for the preparation of the target complexes **1–3** is outlined in eqn. (1). It involves treatment of the corre-



sponding neutral chloro derivatives **4–6**, which contain the μ-η²-Si,O bridge between the metals, with TIPF₆ in the presence of the appropriate P–Z phosphine. The driving force for this reaction is the formation of insoluble TiCl₄. The counter ion PF₆[−] is a reliable probe in ³¹P-¹H} NMR spectroscopy (septuplet centered at ca. δ −144, J_{PF} = ca. 700 Hz). Note that when silver salts were used as halide abstractors secondary reactions led to decomposition products such as [Fe(CO)₃(dppm-P,P')] or [Fe(CO)₃(dppa-P,P')].

Cationic complexes displaying a μ-η²-Si,O bridge

Complexes with EPh₃ (E = P or As) 7,8. We first prepared cations **7** and **8** from EPh₃ (E = P or As) and **4** or **6** eqn. (2), in



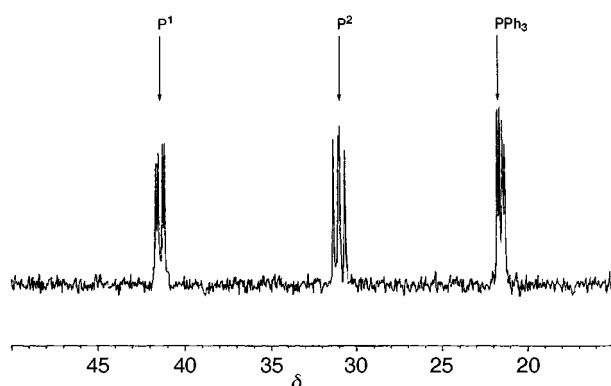
which the Fe–Si–O→Pd four-membered ring is retained. Thus their NMR and IR data could be used for comparison with those of complexes **1–3** and help determine the structures of the latter.

Complex **7a** has been obtained as a red-orange powder in an analytically pure form after a CH₂Cl₂ solution of **4** and PPh₃ was treated with TIPF₆, the volatiles removed *in vacuo* and the residue washed with Et₂O and pentane. In addition to the characteristic PF₆[−] signal (septuplet at δ −143.5, ¹J_{PF} = 710 Hz), the ³¹P-¹H} NMR spectrum consists of three doublets of doublets, the three phosphorus atoms being coupled to each other (Table 1, Fig. 1). The signals at lower field, δ 41.4 and 31.0, are assigned by comparison with **4** to the P atoms of the dppm ligand, P(Fe) and P(Pd), respectively (²⁺³J_{PP} = 45 Hz). The signal at δ 21.5 is ascribed to the PPh₃ ligand (Table 1). In the ¹H NMR spectrum the methoxysilyl ligand gives rise to a very broad signal centered at δ 3.47 as the result of its hemilability and the successive involvement of the different oxygen atoms in co-ordination to the Pd. Upon cooling to 273 K, two

Table 1 Selected $^{31}\text{P}\{-^1\text{H}\}$ NMR and IR data of cationic complexes **7** and **8** and their corresponding neutral complexes **4** and **6**

Complex	Chemical shifts (J/Hz)			Coupling constants/Hz			$\tilde{\nu}(\text{CO})/\text{cm}^{-1}$
	P_{Fe}^a ($J_{\text{P-Pt}}$)	P_{M}^b ($J_{\text{P-Pt}}$)	PPh_3 ($J_{\text{P-Pt}}$)	$J_{\text{P}^1\text{-P}^2}$	$J_{\text{P}^1\text{-P}^3}$	$J_{\text{P}^2\text{-P}^3}$	
4	48.0	34.9		55			1985m, 1925s, 1905s
7a	41.4	31.0	21.5	45	16	42	2000s, 1950m, 1930s
7b	40.1	30.2		47			2004s, 1950m, 1932s
6	52.9	7.7 (4756)		47			1995m, 1935s, 1910s
8a	44.5 (37)	6.4 (4676)	36.5 (2806)	39	13	12	2000s, 1947m, 1916s
8b	44.4 (40)	5.3 (4593)		42			2004s, 1954m, 1925s

^a P atom of the dpmm ligand co-ordinated to the Fe. ^b P atom of the dpmm ligand co-ordinated to the Pd in complex **7** or Pt in **8**. ^c Recorded in CH_2Cl_2 .

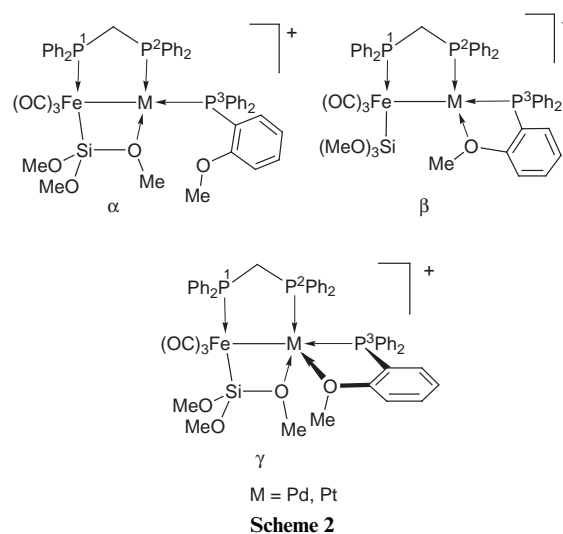
**Fig. 1** The $^{31}\text{P}\{-^1\text{H}\}$ NMR spectrum of the cation in complex **7a**.

signals are observed at δ 3.40 and 3.71 with relative intensities of 2:1 ($\Delta G^\ddagger = 55.6 \pm 1.1 \text{ kJ mol}^{-1}$ for a coalescence temperature of 278 K). In the IR spectrum (CH_2Cl_2) three $\nu(\text{CO})$ absorptions typical for a meridional arrangement of the CO ligands around the iron centre are observed at 2000s, 1950m and 1930s cm^{-1} . These values are at higher wavenumbers than those of neutral **4**, indicating that in **7a** the effect of the positive charge of the complex prevails over the donor properties of the PPh_3 ligand (Table 1). Complex **7b** displays a similar AX pattern in the $^{31}\text{P}\{-^1\text{H}\}$ NMR spectrum and its IR characteristics are similar to those of **7a**. The ^1H NMR spectrum of the former, however, shows for the methoxysilyl ligand two singlets at δ 3.77 and 2.89 with relative intensities of 2:1, the latter being assigned to the three methyl protons of the OMe group co-ordinated to the Pd. In this complex rotation of the silyl ligand about the Fe–Si axis is therefore not observed on the NMR timescale at room temperature. It is interesting to contrast this behaviour with that of **7a** and this may be due to the lower donor ability of AsPh_3 vs. PPh_3 .

The platinum complexes **8** exhibit IR spectra in the $\nu(\text{CO})$ region similar to those of their palladium counterparts **7**, with absorption bands being at higher wavenumbers than in the case of the parent neutral complex **6** (Table 1). In the $^{31}\text{P}\{-^1\text{H}\}$ NMR spectrum of **8a** the chemical shift of PPh_3 is observed at lower field than in **7a** (δ 36.5 vs. 21.5) whereas the $J_{\text{P-P}}$ coupling constants are similar in both cases, except for J_{cis} between the two phosphorus atoms co-ordinated to M: 12 Hz for **8a** (M = Pt) vs. 42 Hz in **7a** (M = Pd). The $^1J_{\text{P-Pt}}$ coupling constants between the different P atoms and Pt are very different: 4676 Hz in the case of the P atom of the dpmm ligand and 2806 Hz in the case of PPh_3 . This should be related to the fact that the former is *trans* to a relatively weak ligand whereas the latter phosphine experiences the *trans* influence of the metal–metal bond. In the ^1H NMR spectra of **8a, 8b** the methoxy protons of the $\text{Si}(\text{OMe})_3$ unit give rise to two singlets in a 1:2 ratio, thus showing the

rigidity of this ligand on the NMR timescale, as already observed for **6**.^{3b}

Dpmm–Fe–Pd and Fe–Pt complexes 1a and 3a with P–Z = $\text{Ph}_2\text{PC}_6\text{H}_4(o\text{-OMe})$. We have been interested in preparing complexes **1a** and **3a** from $\text{Ph}_2\text{PC}_6\text{H}_4(o\text{-OMe})$, since the methoxy donor function thus introduced in the co-ordination sphere of the palladium atom would be of a similar nature to that of the bridging alkoxy-silyl ligand. Depending on whether or not the pre-existent Si–O bridge is retained, isomers α – γ could be envisaged. In the case of isomer β , co-ordination of the oxygen atom of the anisyl group to the Pd or Pt would generate a five-membered ring expected to be thermodynamically more favorable than the Fe–Si–O→Pd four-membered ring retained in isomer α . Furthermore, the possibility of forming isomer γ with a five-co-ordinated centre should also be considered (Scheme 2).



Both the IR and NMR spectra of complex **1a** show great similarities with those of **7a** (see Tables 1–3). In the $^{31}\text{P}\{-^1\text{H}\}$ NMR spectrum the signal assigned to co-ordinated $\text{Ph}_2\text{PC}_6\text{H}_4(o\text{-OMe})$ occurs at δ 14.7. Although it is at higher field than that of PPh_3 in **7a** (δ 21.5), the differences in chemical shifts between “free” and co-ordinated ligands are similar: $\Delta\delta = +27$ and $+30$ for **7a** and **1a**, respectively. In the ^1H NMR spectrum the four methoxy groups give rise to two signals at δ 3.39 and 3.74, with relative intensities of 3:1. The latter is a sharp singlet, assigned to the methyl protons of the anisyl group which does not appear to chelate the Pd since the chemical shift is the same as for the free phosphine. The former signal is broad and ascribed to the three OMe groups of the silyl ligand, which appear equivalent on the NMR timescale, as the result of

Table 2 Selected IR data (cm⁻¹) for the cationic complexes **1** and **2**^a

Complex	$\nu(\text{CO})$, <i>mer</i> -Fe(CO) ₃	Other
1a	1995vs, 1941 (sh), 1918vs	
1b, 1b'	1999vs, 1949 (sh), 1931vs ^b	
1c	2000vs, 1947 (sh), 1925vs	1670s ^c
1d	1992vs, 1944 (sh), 1918vs	
1e	2001vs, 1947 (sh), 1928vs	2258w ^d
1f, 1f'	1992vs, 1945 (sh), 1925vs	1659s, ^c 1591m, ^e 1555m ^e
1g	1978vs, 1925 (sh), 1907vs	
1h	1977vs, 1924 (sh), 1908vs	
2c	2007vs, 1955 (sh), 1942vs	1670s ^c
2g	1977vs, 1924 (sh), 1907vs	
3a	1995vs, 1940 (sh), 1912vs	

^a Recorded as KBr disk. ^b Recorded in CH₂Cl₂. ^c $\nu(\text{CO})$ vibration of the ketone/amide functionality. ^d $\nu(\text{C-N})$ vibration. ^e $\nu(\text{C-N})$ of the amide functionality.

the hemilabile behaviour of this ligand (see above). Variable temperature ¹H NMR experiments confirmed these attributions: the signal at δ 3.39, which is slightly shifted towards lower field upon cooling, splits into two signals at δ 3.60 and 3.79, with relative intensities of 2:1, below coalescence temperature (245 K). The IR and NMR data are thus in favour of a structure for **1a** similar to that of **7a** and only isomer α is observed. Thus competition for co-ordination to palladium between the methoxy groups of the silyl ligand and that of the phosphine Ph₂PC₆H₄(*o*-OMe) is not observed, the Fe-Si-O→Pd four-membered ring remaining entropically favoured. Attempts to obtain suitable crystals of **1a** for X-ray analysis led to the formation of decomposition products, amongst which the new cationic complex [PdCl(dppm-*P, P'*){Ph₂PC₆H₄(*o*-OMe)}]PF₆ **9** and the known but not yet structurally characterized [Pd₂Cl₂(μ -CO)(μ -dppm)₂] **10**.⁷ Both these compounds have been isolated and structurally characterized (see below).

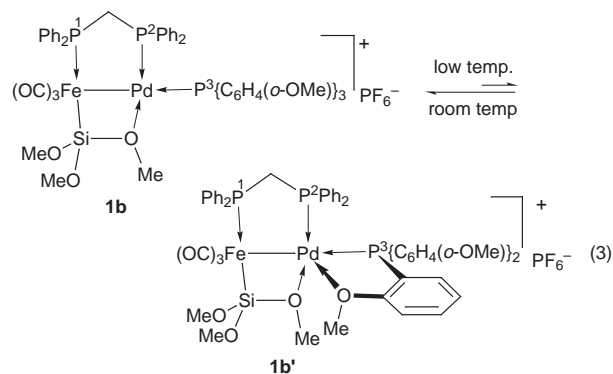
The platinum complex **3a** has also been prepared, from **6** and Ph₂PC₆H₄(*o*-OMe), by using the method described above. Both the IR and NMR data (Tables 2 and 3), which are comparable to those of **1a** and **8,8b**, are consistent with this complex having a structure similar to that of **1a**, with isomer α being the only one observed (Scheme 2).

Note that when CO gas was passed through solutions of these complexes for 15 to 30 min the IR spectra in the $\nu(\text{CO})$ region were not modified; co-ordination of CO was not observed. This is similar to previous observations made on the neutral complexes **4-6**.³

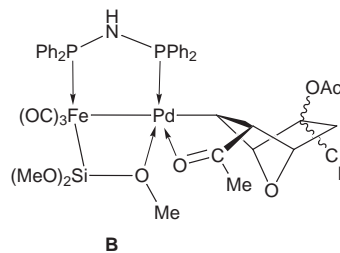
dppm Fe-Pd complex 1b with P-Z = P{C₆H₄(*o*-OMe)}₃. In the $\nu(\text{CO})$ region the IR spectrum of complex **1b** which contains the tris(*o*-anisyl)phosphine shows great similarities with that of **1a** (Table 2). In the room temperature ³¹P-¹H NMR spectrum two doublets of doublets are observed at δ 40.5 (²⁺³J_{P1-P2} = 45 and ³⁺⁴J_{P1-P3} = 16 Hz) and 27.4 (²J_{P2-P3} = 37 Hz), which are ascribed to the P(Fe) and P(Pd) atoms of the dppm ligand, respectively. The signal corresponding to co-ordinated P{C₆H₄(*o*-OMe)}₃ occurs as a very broad signal around δ 0, which hardly emerges from the baseline and suggests a dynamic process. Upon cooling, a splitting of the above resonances was observed and signals corresponding to two isomers **1b** and **1b'**, in a 85:15 ratio, appeared below 263 K (Table 3, Fig. 2). Note that the ¹H NMR spectrum contains complicated sets of signals, in the δ 3.21–3.83 region, due to the numerous methoxy groups. More specific assignments were not attempted.

We have previously reported that ²⁺³J_{P1-P2} values ranged from 40 to 56 Hz for bimetallic complexes stabilized by a Fe-Si-O→M four-membered ring (M = Pd, Pt, *etc.*) and from 80 to 110 Hz in the absence of the latter (this has also been noticed in the present study, see below and Table 3).^{3,8} Thus, the observed

²⁺³J_{P1-P2} values for the two isomers **1b** (45 Hz) and **1b'** (44 Hz) are consistent with the presence of a SiO→Pd interaction in both cases. The only difference between the two ³¹P-¹H NMR AMX spin systems concerns the chemical shifts assigned to the tris(*o*-anisyl)phosphine. In the case of the major isomer **1b**, the $\Delta\delta$ between "free" (δ -39.5) and co-ordinated phosphine is +34.2 ppm. Since this downfield shift is in the same range as that observed for Ph₂PC₆H₄(*o*-OMe) in **1a** or for PPh₃ in **7a**, we suggest for **1b** the same structure as for **1a** and **7a**, the tris(*o*-anisyl)phosphine acting as a monodentate ligand eqn. (3). On

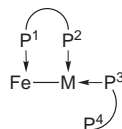


the other hand, in the case of the minor isomer **1b'** the chemical shift of co-ordinated phosphine occurs at lower field than for **1b** ($\Delta\delta$ = +15.5 ppm). This suggests a different co-ordination mode and a possible MeO→Pd interaction involving the phosphine ligand. Chelation of this phosphine to the Pd would generate a P-C-C-O→Pd five-membered ring, eqn. (3), which would contribute to the downfield shift observed. Thus a structure with two O→Pd interactions, involving both the phosphine and the silyl ligand, can be envisaged for **1b'**. We have recently structurally characterized the bimetallic complex [(OC)₃-Fe{ μ -Si(OMe)₂(OMe)}(μ -Ph₂NHPPH₂)Pd{C₆H₉NO₃C(=O)-Me}] **B** in which five-co-ordination of the palladium centre is achieved by dative interactions with the ketone function in the apical position of a square-based pyramid (C=O→Pd 2.769(5) Å) and the alkoxysilyl ligand (SiO→Pd = 2.240(3) Å).^{5e}



Our structural proposal is also consistent with the fact that five- and even six-co-ordinate palladium centres have been reported and that phosphine ligands containing *o*-anisyl groups are commonly used as P,O chelating ligands⁹ (see also below the crystal structure of **9**). Although a crystal structure of complex **1b/1b'** is not available it is reasonable to assume that a species of type **1b'** best represents the static structure of this complex. Modeling studies with Chem3D (see Fig. 3) support this view and indicate that even a six-co-ordinated species might be envisaged since Pd→O distances of 2.553 and 2.825 Å are found (Fig. 3). This suggests a potential, incipient tridentate behaviour for ligand P{C₆H₄(*o*-OMe)}₃.

dppm and dppa Fe-Pd complexes 1c-1e and 2c. The cationic complexes **1c-1e** have been obtained following the same procedure as that described above for the synthesis of **1a**. On the basis of the IR and ³¹P-¹H NMR data, which are given in Tables 2 and 3 respectively, it appears that the ketone or alkene

Table 3 $^{31}\text{P}\{-^1\text{H}\}$ NMR data (δ , J/Hz) of cationic complexes^a

Complex	P ¹	P ²	P ³	P ⁴	²⁺³ J _{P¹-P²}	³⁺⁴ J _{P¹-P²}	² J _{P²-P³}	³⁺⁴ J _{P¹-P⁴}	² J _{P²-P⁴}	² J _{P³-P⁴}
1a	41.5	28.5	14.7		45	23	40			
1b ^b	40.8	28.8	-5.3		45	16	33			
1b' ^b	42.0	26.8	10.2		44	15	31			
1c	40.1	25.6	6.7		47	14	40			
1d	41.7	29.4	12.8		45	16	40			
1e	39.4	26.4	9.4		46	14	44			
1f	40.4	25.7	10.6		44	13	41			
1f'	66.1	30.6	52.9		45	18	27			
1g	64.4	23.1	124.6	90.7	85	70	30	27	535	90
1h	64.6	25.4	124.9	92.2	81	71	33	27	536	94
2c	94.2	78.2	5.6		41	13	46			
2g	108.0	70.5	45.5	50.5	85	10	12	30	506	105
3a	43.9 ^c	4.3 ^d	33.1 ^e		41	13	^f			

^a In CD₂Cl₂; P¹, P², P³ and P⁴ refer to the different phosphorus atoms in complexes **1** and **2**. ^b Recorded at 243 K. ^c ¹J_{P-Pt} not observed. ^d ¹J_{P-Pt} = 4747 Hz. ^e ¹J_{P-Pt} = 2862 Hz. ^f Not observed.

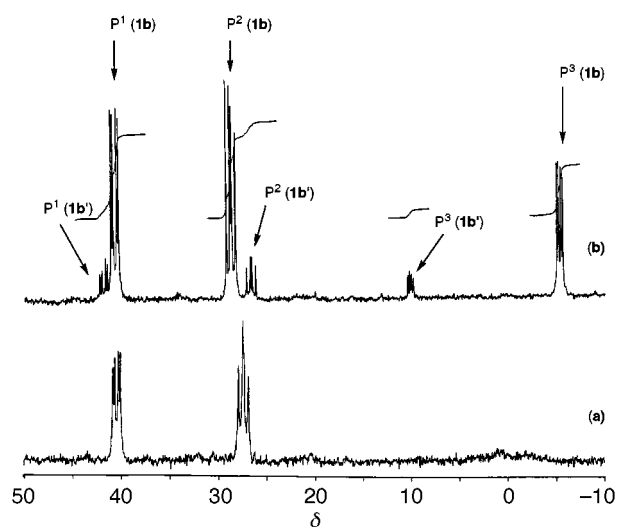


Fig. 2 The $^{31}\text{P}\{-^1\text{H}\}$ NMR spectra of the cation in complex **1b/1b'** at (a) 298 K, (b) 243 K in CD₂Cl₂.

functionality does not co-ordinate to the palladium centre, neither by displacing the Fe–Si–O→Pd four-membered ring nor by giving a five-co-ordinated species. Indeed, in both cases, the ¹H NMR spectrum shows two signals for the alkoxy-silyl protons in a 2:1 ratio, indicating the non-equivalence of the OMe groups and the persistence of the SiO bridge between the Fe and Pd. For **1c** the $\nu(\text{C}=\text{O})$ absorption of the ketone function (1670 cm⁻¹) is identical to that of the free phosphine, whereas chelation of Ph₂PCH₂C(O)Ph to palladium usually causes a shift towards lower wavenumbers by ca. 100 cm⁻¹.¹⁰ Similarly the phosphinonitrile Ph₂PCH₂CH₂CN behaves as a monodentate ligand in complex **1e** in which the $\mu\text{-}\eta^2\text{-Si}_2\text{O}$ bridge is retained. The $\nu(\text{CN})$ vibration is observed at the same value (2258 cm⁻¹) as for the unco-ordinated phosphine.

In order to evaluate the influence of chemical modifications in the assembling ligand, we have prepared the Ph₂PNHPPPh₂ (dppa) complex **2c**, from **5** and Ph₂PCH₂C(O)Ph. The spectroscopic data are given in Tables 2 and 3. In the $^{31}\text{P}\{-^1\text{H}\}$ NMR spectrum the two signals at lower field δ 94.2 and 78.2 are assigned to the P(Fe) and P(Pd) atoms of the dppa ligand, respectively. By comparison with neutral **5**, a slight upfield shift of ca. 6 ppm is noticed for these two signals, as in the dppm series (Tables 1 and 3). In the IR spectrum, the $\nu(\text{C}=\text{O})$ absorption of the ketone is observed at 1670 cm⁻¹, as for Ph₂PCH₂-

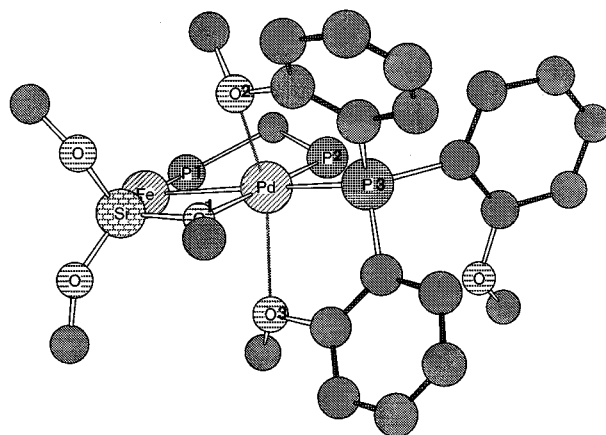


Fig. 3 Chem3D model of complex **1b'** produced by using the following parameters inspired by the structure determination of [(OC)₃-Fe{ $\mu\text{-Si}(\text{OMe})_2(\text{OMe})$ }($\mu\text{-dppm})$ PdSnPh₃]^{3c} or of **9** (for Pd–P(3)): Pd–P(2) 2.19, Pd–P(3) 2.370, Pd–Fe 2.670, Pd–O(1) 2.148, Pd–O(2) 2.825, Pd–O(3) 2.553, Fe–Si 2.260, Fe–P(1) 2.200, Si–O(1) 1.685, O(1)–C 1.38, O(2)–C 1.38, O(3)–C 1.38 Å; Si–Fe–P(1) 171.0, Si–O(1)–Pd 96.7, O(1)–Pd–P 175.0, Fe–Pd–P(2) 175.0, P(2)–Pd–P(3) 93.0°.

C(O)Ph. Here again, the ketone functionality in **2c** does not displace the SiO→Pd interaction.

dppm Complex 1f (P–Z = Ph₂PCH₂C(O)NPh₂). The NMR and IR data of cation **1f** which contains an amidophosphine ligand being similar to those of **1c** (Tables 2 and 3), we assume that their structures are comparable. However, **1f** was accompanied by a second species **1f'** (ratio **1f**:**1f'** = 70:30) which displays in the ^{31}P NMR spectrum a set of three doublets of doublets, at lower field than those of **1f** (Table 3 and Fig. 4). The main feature is the large downfield shifts, compared with **1f**, observed for the signals (a) of the P atom of the dppm ligand co-ordinated to the iron centre (+25.7 ppm) and (b) of Ph₂PCH₂C(O)NPh₂ (+42.3 ppm).

The IR spectrum shows an additional $\nu(\text{C}=\text{O})$ vibration at 1555 cm⁻¹, which may be assigned to an amide function co-ordinated by its O atom to the electron deficient Pd.¹¹ The ¹H NMR spectrum of the mixture **1f**, **1f'** contains three signals in a 4:1:1 ratio at δ 3.74, 3.58 and 3.55, respectively, for the OMe protons. This would be consistent with the presence of two isomers containing a $\mu\text{-}\eta^2\text{-Si}_2\text{O}$ bridging interaction. Therefore on the basis of the spectroscopic data, we propose that in **1f'** the functional phosphine ligand Ph₂PCH₂C(O)NPh₂

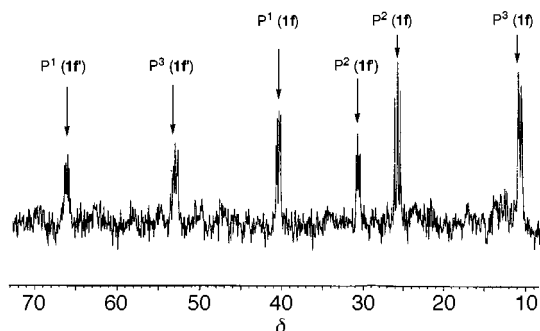
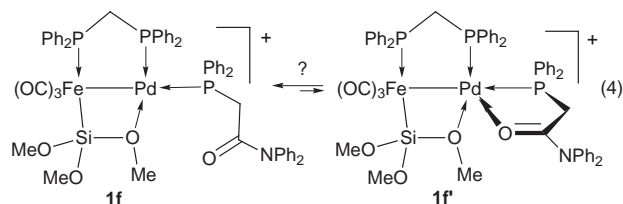


Fig. 4 The $^{31}\text{P}\{-^1\text{H}\}$ NMR spectrum of the cation in complex **1f/1f'**.

chelates the Pd and affords a five-co-ordinated species. This is supported by observations made with related, structurally characterized Fe–Pd complexes in which a ketone function acts as a fifth ligand toward the Pd.^{5e} Clearly, the protons of the SiOMe bridge are more sensitive to the change in co-ordination at the palladium than those of the other methoxy groups which resonate at δ 3.74 in both cases. The two isomers **1f**, **1f'** could not be separated, perhaps owing to the existence of an equilibrium of the type (4), which would be slow on the NMR



timescale since no dynamic behaviour was observed by VT NMR within the stability range of the complex (<323 K). The contrasting behaviour of $\text{Ph}_2\text{PCH}_2\text{C}(\text{O})\text{Ph}$ and $\text{Ph}_2\text{PCH}_2\text{C}(\text{O})\text{NPh}_2$ may be due to the slightly better donor properties of the amide *vs.* the ketone function.¹¹

Cationic complexes in which the $\mu\text{-}\eta^2\text{-Si,O}$ bridge is displaced

dppm Complexes 1g, 1h ($\text{P-Z} = \text{Ph}_2\text{PN}(\text{R})\text{PPh}_2$). Diphosphines such as dppm or dppa also appeared to be interesting candidates for competition with the $\text{SiO} \rightarrow \text{Pd}$ bond. However, despite numerous attempts, reactions of complex **4** with dppm or dppa in the presence of an halide abstractor led to decomposition and/or mixtures of products; the desired complexes were not detected. Reasons for these observations remain speculative although in the case of dppa its low solubility may represent a drawback. In order to circumvent this problem we have used the more soluble *N*-methyl derivative $(\text{Ph}_2\text{P})_2\text{NMe}$.

Preliminary observations revealed that in the absence of halide abstractor complex **4** reacted with $(\text{Ph}_2\text{P})_2\text{NMe}$ to yield decomposition products, probably owing to displacement of the Pd-bound dppm P atom by $(\text{Ph}_2\text{P})_2\text{NMe}$. In order to prevent this pathway, **4** was first treated with TIPF_6 in acetonitrile, below 273 K, to generate *in situ* $[(\text{OC})_3\text{Fe}\{\mu\text{-Si}(\text{OMe})_2(\text{OMe})\}(\mu\text{-dppm})\text{Pd}(\text{NCMe})]\text{PF}_6$ before the phosphine was added. The latter displaced the acetonitrile ligand, which afforded **1g** as the sole product (see Scheme 3). Its $^{31}\text{P}\{-^1\text{H}\}$ NMR spectrum shows, apart from the signal due to PF_6^- , four signals, two for each of the diphosphine ligands. The pattern of these signals, doublets of doublets of doublets, indicates that all the phosphorus atoms are coupled to each other (Table 3, Fig. 5). The signals at δ 124.6 (P^3) and 90.7 (P^4) are assigned to the P atoms of ligand $(\text{Ph}_2\text{P})_2\text{NMe}$, whereas the two signals at higher field, δ 64.4 (P^1) and 23.1 (P^2), are ascribed to the P atoms of the bridging dppm ligand, P(Fe) and P(Pd) respectively. In comparison with complexes **1a**, **1c–1f**, the P(Fe)

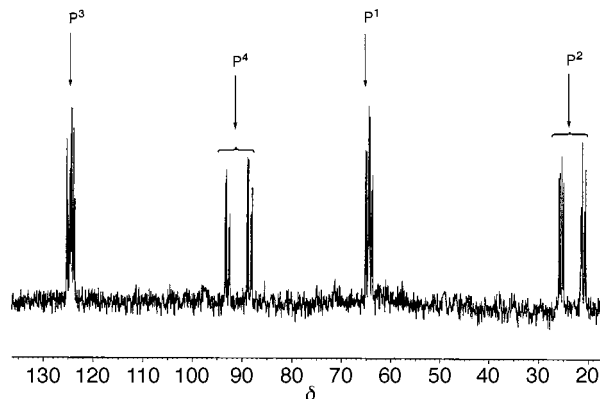
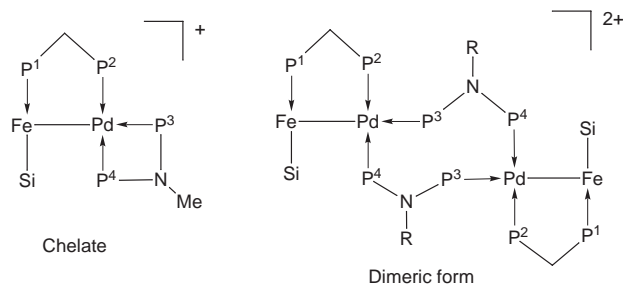


Fig. 5 The $^{31}\text{P}\{-^1\text{H}\}$ NMR spectrum of the cation in complex **1g**.

signal is shifted towards lower field by *ca.* 24 ppm, whereas the P(Pd) signal is shifted in the opposite direction. These observations indicate for **1g** a different structure. The most striking feature is the very large $J_{\text{P-P}}$ value of 535 Hz between P^2 and P^4 , which indicates a *trans* disposition of these two atoms. In the ^1H NMR spectrum the nine methoxy protons appear equivalent since a sharp singlet is observed at δ 3.59. In the IR spectrum of **1g** the $\nu(\text{CO})$ vibrations occur at lower wavenumbers than for **1a**, **1c–1f** (Table 2), thus indicating a higher electron density in the former. This would be expected if the two phosphorus atoms of ligand $(\text{Ph}_2\text{P})_2\text{NMe}$ were co-ordinated to the Pd. On the basis of these spectroscopic data, we therefore conclude that the $\text{SiO} \rightarrow \text{Pd}$ interaction has been displaced. Nevertheless, a chelating co-ordination mode for $(\text{Ph}_2\text{P})_2\text{NMe}$, as depicted in Scheme 3, is not corroborated by the observed ^{31}P NMR



Scheme 3 Representations of structures discussed for complexes **1g, 1h** (phenyl, carbonyl and methoxy groups have been omitted for clarity).

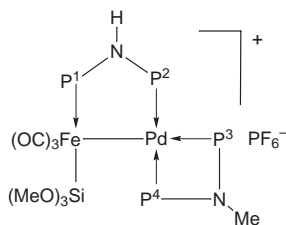
chemical shifts (δ 124.6 and 90.7). In such a case, these should be high field shifted in comparison to that of unco-ordinated $(\text{Ph}_2\text{P})_2\text{NMe}$ (δ 72), owing to the chelate effect.¹² The data are more in accordance with a bridging co-ordination mode of ligand $(\text{Ph}_2\text{P})_2\text{NMe}$ between two Pd, one of the P atoms (P^3) being *trans* to the Fe–Pd bond in one bimetallic unit, the other one (P^4) being *trans* to the P^2 atom of the dppm ligand in another bimetallic unit. The exact structure of **1g** could not be determined by X-ray analysis, since, as for the other cationic bimetallic complexes described above, suitable crystals could not be obtained owing to slow decomposition in solution. However, mass spectroscopy using electrospray (**1g**) or FAB^+ (**1h**) techniques showed the presence of isotopic patterns consistent with dinuclear Fe–Pd monocationic and tetranuclear Fe_2Pd_2 dicationic species. The latter is best explained by a dimeric form for these complexes (Scheme 3). Higher nuclearity cyclic species could be envisaged but were not detected.

With the combined objectives of confirming the above observations and of obtaining complexes of potential use in sol–gel processes, we have prepared complex **1h** from **4** and the phosphine $(\text{Ph}_2\text{P})_2\text{N}\{(\text{CH}_2)_3\text{Si}(\text{OEt})_3\}$, following the same procedure as for **1g**. Complex **1h** was obtained as a burgundy-red powder. Both its IR and NMR data are similar to those of

1g (Tables 2 and 3), thus indicating a similar structure (Scheme 3). The ^1H NMR spectrum shows the expected signals for the $(\text{CH}_2)_3\text{Si}(\text{OEt})_3$ moiety.

dppa Complex 2g ($\text{P-Z} = \text{Ph}_2\text{PN}(\text{Me})\text{PPh}_2$). For comparison, we have also prepared the dppa analogue of complex **1g** from **5** and phosphine $(\text{Ph}_2\text{P})_2\text{NMe}$. The IR spectrum of this new complex is similar to that of **1g**, **1h** in the $\nu(\text{CO})$ region (Table 2). In the $^{31}\text{P}\{-^1\text{H}\}$ NMR spectrum the P(Fe) and P(Pd) signals of the bridging dppa ligand appeared at lower and higher field, respectively, than for **2c** (Fig. 6). Similar trends were observed between the dppm complexes **1a**, **1c–1f** and **1g**, **1h** (see above). The similarity between the $^{2+3}J_{\text{P}1,\text{P}2}$ values of 81–85 Hz for **2g** and **1g**, **1h** is noteworthy and contrasts with those for the other cationic complexes where they range from 41 to 47 Hz. This would suggest the absence of a $\mu\text{-}\eta^2\text{-Si}_2\text{O}$ bridge in the former, by analogy with observations made previously with related, neutral bimetallic complexes.^{3,8}

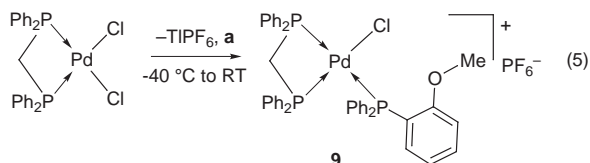
Interestingly, the signals assigned to co-ordinated $(\text{Ph}_2\text{P})_2\text{NMe}$ occurred at δ 45.5 (P^3) and 50.5 (P^4) (Fig. 6), at high field compared to that of the “free” phosphine (δ 72), and thus suggest a chelating co-ordination mode for this ligand. This contrasts with the situation in **1g** where the phosphine does not chelate but acts as a bridging ligand. Furthermore, for both mononuclear neutral and cationic palladium complexes in which $(\text{Ph}_2\text{P})_2\text{NMe}$ has been found to chelate the metal centre, the ^{31}P NMR chemical shifts also occurred in the δ 40–50 region.¹⁵ That the $J_{\text{P}1,\text{P}3}$ and $J_{\text{P}2,\text{P}3}$ values are much smaller for **2g** than for **1g**, **1h** (Table 3) is again consistent with different structures for these complexes. The *trans* arrangement of P^2 and P^4 is confirmed by the large coupling constant between these two nuclei (506 Hz).



Clearly, the co-ordination mode of $(\text{Ph}_2\text{P})_2\text{NMe}$ is strongly influenced by the nature of the assembling ligand (dppm or dppa). Unfortunately, the reactions of **5** with dppa or dppm carried out for comparison did not allow isolation of any well defined complex.

Crystal structures of complexes **9** and **10**

X-Ray quality crystals of complexes **9** and **10** were obtained from adventitious decomposition of **1a** in a CH_2Cl_2 –toluene–hexane mixture. However, **9** was then prepared in a rational way (62% yield) by treatment of a mixture of $[\text{PdCl}_2(\text{dppm}-P,P')]$ and $\text{Ph}_2\text{PC}_6\text{H}_4(o\text{-OMe})$ with TlPF_6 , eqn. (5), whereas **10** is easily prepared by carbonylation of $[\text{Pd}_2\text{Cl}_2(\mu\text{-dppm})_2]$.⁷



The molecular structure of the cation of complex **9** is shown in Figs. 7 and 8 and selected bond distances and angles are listed in Table 4. The Pd atom has a square planar co-ordination environment involving the Cl and the three P atoms. The bond distances to Pd are in the normal range. The Pd–P(3) distance of 2.372(1) Å is slightly longer than the Pd–P(1) (2.281(1) Å) and Pd–P(2) (2.262(1) Å) distances involving the P

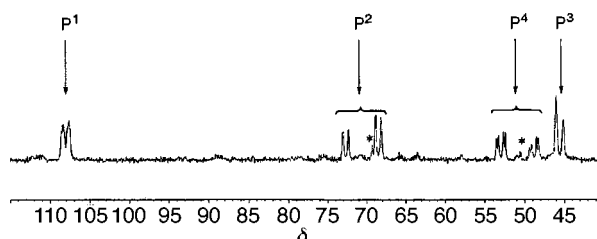


Fig. 6 The $^{31}\text{P}\{-^1\text{H}\}$ NMR spectrum of the cation in complex **2g** (* denotes minor impurities).

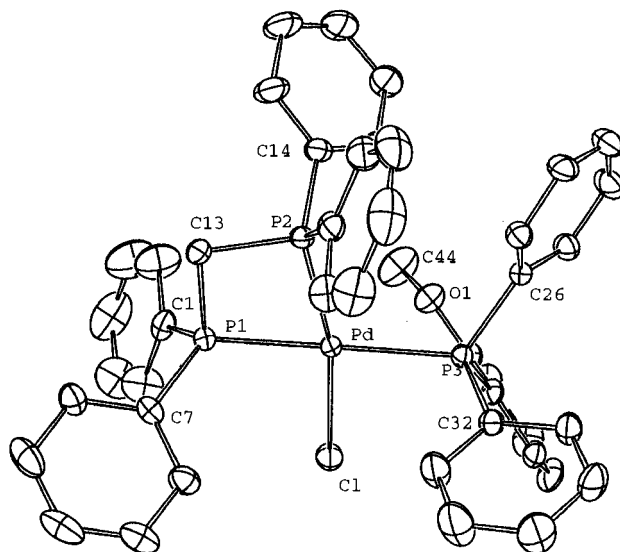


Fig. 7 An ORTEP¹⁴ view of the structure of the cation in complex **9**. Thermal ellipsoids are drawn at the 50% probability level.

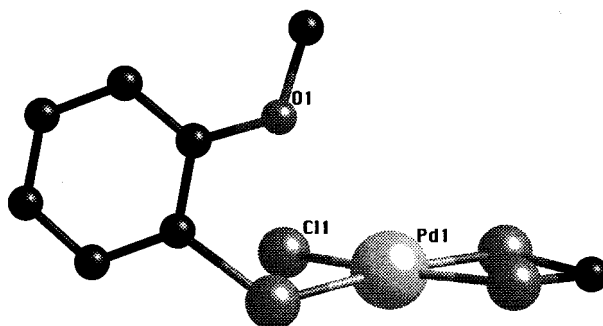


Fig. 8 View of the palladium environment in complex **9** illustrating incipient five-co-ordination (see text).

atoms of the chelating dppm ligand. The methoxy oxygen atom is oriented towards the metal centre, almost residing in an apical position, with a Pd–P(3)–C(38) angle of 108.8(1)° and a P(3)–C(38)–C(39)–O(1) torsion angle of 1.0(5)°. This leads to a pseudo-five-co-ordinated palladium complex, with a long range Pd...O interaction (3.172(3) Å).

Although complex **10** has been known since 1978,⁷ it has not been characterized by X-ray diffraction. Its molecular structure is shown in Fig. 9 and belongs to the expected “A frame” type¹⁵ in which the two palladium centres are held together by mutually *trans* dppm ligands and share a common carbonyl ligand. Selected bond angles and distances are given in Table 4 and lie within the range of those found for related systems such as $[\text{Pd}_2\text{Cl}_2(\mu\text{-CO})(\text{dmpm})_2]$ ($\text{dmpm} = \text{Me}_2\text{PCH}_2\text{PMe}_2$),¹⁶ $[\text{Pd}_2\text{Cl}_2(\mu\text{-CO})(\text{dam})_2]$ ($\text{dam} = \text{Ph}_2\text{AsCH}_2\text{AsPh}_2$),¹⁷ $[\text{Pd}_2\text{Cl}_2(\mu\text{-SO})(\text{dppm})_2]$,¹⁷ $[\text{Pd}_2\{\text{OC}(\text{O})\text{CF}_3\}_2(\mu\text{-CO})(\text{dppm})_2]$ ¹⁸ or $[\text{Pd}_2\text{Cl}_2(\mu\text{-CH}_2)(\text{dmpm})_2]$.¹⁹ The Pd...Pd separation of 3.190 Å suggests no direct metal–metal interaction. There is a slight deviation from square geometry around the almost planar Pd atoms, as shown by the P(1)–Pd(1)–P(3) and P(2)–Pd(2)–P(4)

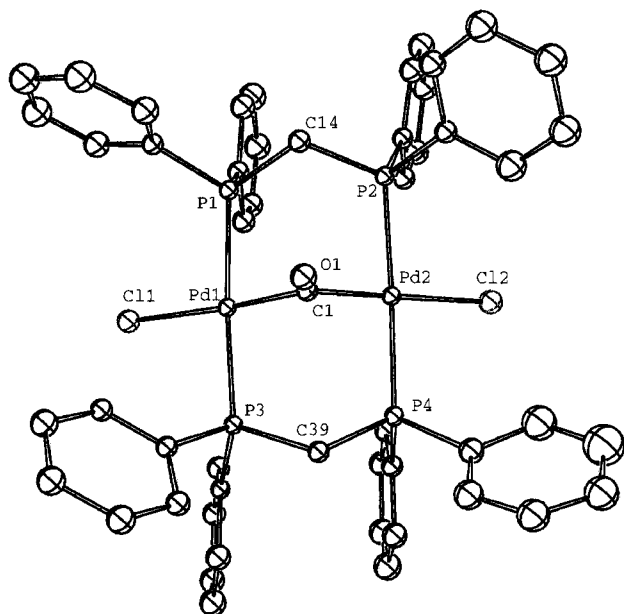


Fig. 9 An ORTEP view of the structure of complex 10. Thermal ellipsoids are drawn at the 30% probability level.

Table 4 Selected bond distances (Å) and angles (°) for complexes 9 and 10

9		10	
Pd–Cl	2.3344(8)	Pd(1)–Cl(1)	2.445(1)
Pd–P(1)	2.2804(7)	Pd(1)–C(1)	1.974(4)
Pd–P(2)	2.2617(7)	Pd(1)–P(1)	2.340(1)
Pd–P(3)	2.3724(7)	Pd(1)–P(3)	2.341(1)
P(1)–C(13)	1.893(3)	Pd(2)–Cl(2)	2.427(1)
P(2)–C(13)	1.835(3)	Pd(2)–C(1)	1.971(4)
C(39)–O	1.356(4)	Pd(2)–P(2)	2.335(1)
O–C(44)	1.413(5)	Pd(2)–P(4)	2.336(1)
		C(1)–O	1.184(5)
		Pd(1)⋯Pd(2)	3.190(4)
Cl–Pd–P(1)	92.85(3)	Cl(1)–Pd(1)–C(1)	174.8(1)
Cl–Pd–P(2)	166.18(3)	P(1)–Pd(1)–Pd(3)	171.48(4)
Cl–Pd–P(3)	89.39(3)	Pd(1)–C(1)–O	125.27(5)
P(1)–Pd–P(2)	73.34(3)	P(1)–Pd(1)–C(1)	86.5(1)
P(1)–Pd–P(3)	174.55(3)	P(3)–Pd(1)–C(1)	85.8(1)
P(2)–Pd–P(3)	104.34(3)	Cl(2)–Pd(2)–C(1)	178.8(1)
P(1)–C(13)–P(2)	95.2(1)	P(2)–Pd(2)–P(4)	171.33(4)
Pd–P(3)–C(38)	108.76(3)	Pd(2)–C(1)–O	126.79(5)
C(38)–C(39)–O(1)	115.0(3)	P(2)–Pd(2)–C(1)	86.1(1)
C(39)–O(1)–C(44)	120.3(3)	P(4)–Pd(2)–C(1)	87.1(1)
		Pd(1)–C(1)–Pd(2)	107.93(5)

angles of 171.48(4) and 171.33(4)°, respectively. The bridging CO is symmetrically bound to the metal atoms, with bond distances Pd(1)–C(1) 1.974(4) and Pd(2)–C(1) 1.971(4) Å and bond angles Pd(1)–C(1)–O 125.27(5), Pd(2)–C(1)–O 126.79(5) and Pd(1)–C(1)–Pd(2) 107.93(5)°. The C(1)–O distance is 1.184(5) Å. The Pd–Cl distances of 2.445(1) and 2.427(1) Å are within the same range as those found in [Pd₂Cl₂(μ-CO)(dmpm)₂] (2.444 and 2.446 Å)¹⁶ and [Pd₂Cl₂(μ-CH₂)(dmpm)₂] (2.429 and 2.419 Å)¹⁹ and slightly longer than those in [Pd₂Cl₂(dpmMe)₂] (dpmMe = Ph₂PCH(Me)PPh₂) (2.420 and 2.401 Å) in which the Cl atoms are *trans* to the Pd–Pd bond.²⁰

Conclusion

In order to study the availability of the masked co-ordination site on the palladium centre in bimetallic complexes containing a bridging μ-η²-Si(OMe)₃ ligand, such as 4 and 5, we have examined the behaviour of various donor functions held in proximity to the palladium centre by a phosphorus donor atom. We have found that donor functionalities such as methoxy,

ketone, amide, olefin or nitrile, present in phosphines, do not displace the pre-existent Fe–Si–O→Pd four-membered ring. With the ligands tris(*o*-anisyl)phosphine and the amidophosphine Ph₂PCH₂C(O)NPh₂, an additional interaction between an oxygen donor and palladium was evidenced, leading to incipient five- or even six-co-ordination in the case of P{C₆H₄(*o*-OMe)}₃.

It is notable that the ligands (Ph₂P)₂NMe and (Ph₂P)₂N{(CH₂)₃Si(OEt)₃} are able to displace the SiO→Pd interaction. The nature of the resulting product depends upon the assembling ligand since with dppm these ligands assume a bridging behaviour whereas with dppa chelation is observed. These features might be related to the dppa ligand being less electron donating than dppm.^{4h}

Experimental

General procedures

All the reactions and manipulations were carried out under an inert atmosphere of purified nitrogen using standard Schlenk tube techniques. Nitrogen (Air liquide, R-grade) was passed through BASF R3-11 catalyst and 4 Å molecular sieves columns to remove residual oxygen and water. Solvents were dried and distilled under nitrogen before use: pentane, hexane and toluene over sodium, tetrahydrofuran and diethyl ether over sodium–benzophenone, acetonitrile and dichloromethane over calcium hydride. Elemental C, H and N analyses were performed by the Service de microanalyses du CNRS. Infrared spectra were recorded on a Bruker IFS 66 FT-IR spectrometer in the 4000–400 cm⁻¹ region and on a Bruker IFS 113V FT-IR spectrometer in the 500–90 cm⁻¹ region. ¹H, ³¹P-¹H and ¹³C-¹H NMR spectra at 300.1, 121.5 and 75.5 MHz, respectively, on a Bruker AM300 instrument. Phosphorus chemical shifts were externally referenced to 85% H₃PO₄ in water with down-field chemical shifts reported as positive.

Preparations

The heterobimetallic complexes 4 and 6^{3b} and the ligands Ph₂PCH₂C(O)Ph,¹⁰ Ph₂PCH₂C(O)NPh₂,¹¹ (Ph₂P)₂NMe,²¹ (Ph₂P)₂N{(CH₂)₃Si(OEt)₃}²² and Ph₂P(CH₂)₂CN²³ were prepared according to published procedures. The ligand Ph₂P{C₆H₄(*o*-OMe)} was obtained by treatment of Ph₂PCl with MgBr{C₆H₄(*o*-OMe)} whereas P{C₆H₄(*o*-OMe)}₃ was purchased from Lancaster Ltd and used without purification.

[(OC)₃Fe{μ-Si(OMe)₂(OMe)}(μ-dppm)Pd{Ph₂P(C₆H₄*o*-OMe)}]₃PF₆ 1a. A solution of complex 4 (225 mg, 0.286 mmol) and Ph₂P{C₆H₄(*o*-OMe)} (87 mg, 0.300 mmol) in 20 ml of CH₂Cl₂ was stirred for 5 min at room temperature. It was then cooled to –30 °C and TlPF₆ (120 mg, 0.343 mmol) added. The reaction mixture was allowed to return slowly to ambient under vigorous stirring. Meanwhile the initial orange colour turned dark red and TlCl precipitated. After filtration over a Celite pad, the solvent was removed under reduced pressure. The residue was washed with diethyl ether (2 × 20 ml) and pentane (2 × 20 ml) and then vacuum dried. Complex 1a was obtained as a red powder in 71% yield (240 mg) (Found: C, 50.64; H, 4.10. C₅₀H₄₈F₆FeO₇P₄PdSi requires C, 50.50; H, 4.07%). ¹H NMR (CD₂Cl₂, 300 MHz, 298 K): δ 3.39 (s, 9 H, Si(OMe)₃), 3.74 (s, 3 H, OMe phosphine), 4.33 (t, 2 H, PCH₂P, ²J_{PH} = 11 Hz) and 6.5–7.5 (m, 34 H, aromatics).

[(OC)₃Fe{μ-Si(OMe)₂(OMe)}(μ-dppm)Pd{P(C₆H₄*o*-OMe)}]₃PF₆ 1b and 1b'. Treatment of complex 4 (100 mg, 0.13 mmol) with P{C₆H₄(*o*-OMe)}₃ (50 mg, 0.14 mmol) and TlPF₆ (52 mg, 0.15 mmol), according to the procedure described for 1a, afforded a red powder, in 81% yield (132 mg) consisting of a mixture of 1b and 1b' (see text) (Found: C, 47.96; H, 4.16. C₅₂H₄₂F₆FeO₇P₄PdSi·CH₂Cl₂ requires C, 47.72;

H, 4.08%). $^1\text{H NMR}$ (CD_2Cl_2 , 300 MHz, 298 K): δ 3.21, 3.25, 3.40, 3.60, 3.75 and 3.83 (18 H, OMe), 4.15 (broad, 2 H, PCH_2P) and 6.4–8.1 (m, 32 H, aromatics).

[(OC)₃Fe{ μ -Si(OMe)₂(OMe)}(μ -dppm)Pd{Ph₂PCH₂C(O)-Ph}]PF₆ 1c. Complex **1c** was prepared as described for **1a** from 500 mg of **4** (0.635 mmol), 195 mg of Ph₂PCH₂C(O)Ph (0.640 mmol) and 250 mg of TlPF₆ (0.716 mmol). It was obtained as a red-orange powder in 78% yield (595 mg) (Found: C, 51.11; H, 4.08. C₅₁H₄₈F₆FeO₇P₄PdSi requires C, 51.00; H, 4.08%). $^1\text{H NMR}$ (CD_2Cl_2 , 300 MHz, 298 K): δ 3.45 (s, 6 H, Si(OMe)₂), 3.55 (d, 2 H, PCH₂C(O), $^2J_{\text{PH}} = 11$), 3.73 (s, 3 H, MeO→Pd), 4.26 (t, 2 H, PCH₂P, $^2J_{\text{PH}} = 10$ Hz) and 6.5–7.9 (m, 35 H, aromatics).

[(OC)₃Fe{ μ -Si(OMe)₂(OMe)}(μ -dppm)Pd(Ph₂PCH₂CH=CH₂)]PF₆ 1d. Complex **1d** was prepared as described for **1a** from 250 mg of **4** (0.317 mmol), 75 mg of Ph₂PCH₂CH=CH₂ (0.33 mmol) and 130 mg of TlPF₆ (0.37 mmol). It was obtained as a burgundy-red powder in 75% yield (268 mg) (Found: C, 49.67; H, 4.02. C₄₆H₄₇F₆FeO₆P₄PdSi requires C, 49.15; H, 4.21%). $^1\text{H NMR}$ (CD_2Cl_2 , 300 MHz, 298 K): δ 2.56 (dd, 2 H, PCH₂C, $^2J_{\text{PH}} = 8$ or 6, $^3J_{\text{HH}} = 6$ or 8 Hz), 3.50 (s, 3 H, MeO→Pd), 3.58 (s, 6 H, Si(OMe)₂), 4.25 (t, 2 H, PCH₂P, $^2J_{\text{PH}} = 11$), 4.99 (dd, 1 H, CH=CH^AH^B, $^3J_{\text{HHtrans}} = 18$, $^2J_{\text{H^AH^{B}}}$ = 2.5), 5.16 (dd, 1 H, CH=CH^AH^B, $^3J_{\text{HHcis}} = 11$, $^2J_{\text{H^AH^{B}}}$ = 2.5 Hz), 5.63 (m, 1 H, CH=) and 6.8–7.8 (m, 30 H, aromatics).

[(OC)₃Fe{ μ -Si(OMe)₂(OMe)}(μ -dppm)Pd(Ph₂PCH₂CH₂-CN)]PF₆ 1e. This complex was prepared as described for **1a** from 250 mg of **4** (0.317 mmol), 79 mg of Ph₂PCH₂CH₂CN (0.33 mmol) and 130 mg of TlPF₆ (0.37 mmol). It was obtained as a red powder in 85% yield (320 mg) (Found: C, 48.91; H, 4.12; N 1.49. C₄₆H₄₅F₆FeNO₆P₄PdSi requires C, 48.63; H, 3.99; N, 1.23%). $^1\text{H NMR}$ (CD_2Cl_2 , 300 MHz, 298 K): δ 1.62 (m, 2 H, PCH₂), 2.08 (m, 2 H, PCH₂CH₂), 3.49 (s, 6 H, Si(OMe)₂), 3.57 (s, 3 H, MeO→Pd), 4.36 (t, 2 H, PCH₂P, $^2J_{\text{PH}} = 11$ Hz) and 7.0–7.7 (m, 30 H, aromatics).

[(OC)₃Fe{ μ -Si(OMe)₂(OMe)}(μ -dppm)Pd{Ph₂PCH₂C(O)-NPh₂}]PF₆ 1f and 1f'. Treatment of 300 mg of complex **4** (0.38 mmol) with 154 mg of Ph₂PCH₂C(O)NPh₂ (0.39 mmol) and 140 mg of TlPF₆ (0.40 mmol), according to the procedure described for **1a**, afforded a red powder in 72% yield (353 mg) consisting of a mixture of **1f** and **1f'** (see text) (Found: C, 53.14; H, 4.46; N, 1.23. C₅₇H₅₄F₆FeNO₇P₄PdSi requires C, 52.94; H, 4.21; N, 1.08%). $^1\text{H NMR}$ (CD_2Cl_2 , 300 MHz, 298 K): δ 3.45 (d, PCH₂C(O), $^2J_{\text{PH}} = 7$), 3.55 (s, OMe), 3.58 (s, OMe), 3.74 (s, OMe), 3.95 (t, PCH₂P, $^2J_{\text{PH}} = 10$), 4.08 (d, PCH₂C(O), $^2J_{\text{PH}} = 10$), 4.27 (t, PCH₂P, $^2J_{\text{PH}} = 12$ Hz) and 6.6–7.7 (m, 35 H, aromatics).

[(OC)₃{(MeO)₃Si}Fe(μ -dppm)Pd{Ph₂PN(Me)PPh₂}]_n[PF₆]_m 1g. A solution of complex **4** (150 mg, 0.19 mmol) in 20 ml of MeCN was cooled to -40°C and TlPF₆ (70 mg, 0.20 mmol) added. The resulting suspension was stirred for 1 h while the temperature was maintained below -30°C . Then solid (Ph₂P)₂NMe (80 mg, 0.20 mmol) was added, the temperature was allowed to warm to ambient and the mixture further stirred for 14 h. The initial orange-red colour turned dark red and TiCl₄ precipitated. After filtration over a Celite pad, the solvent was removed under reduced pressure and the residue extracted with CH₂Cl₂. The filtrate was dried *in vacuo*, affording a red-brown sticky material which was washed with diethyl ether (10 ml) and pentane (2 × 10 ml) and then vacuum dried. Complex **1g** was obtained as a red-brown powder in 58% yield (143 mg) (Found: C, 49.50; H, 4.09; N, 1.27. C₅₆H₅₄F₆FeNO₆P₅PdSi·

CH₂Cl₂ requires C, 49.89; H, 4.20; N, 1.08%). $^1\text{H NMR}$ (CD_2Cl_2 , 300 MHz, 298 K): δ 2.47 (s, 3 H, NMe), 3.59 (s, 9 H, Si(OMe)₃), 3.74 (t, 2 H, PCH₂P, $^2J_{\text{PH}} = 11$ Hz) and 6.6–7.9 (m, 40 H, aromatics). Mass spectrum (electrospray, acetonitrile, 40 V): m/z 1066.0 ($\text{M}^+ - \text{PF}_6 - 3\text{CO}$, 100), 705.8 [$2(\text{M}^+) - 2\text{PF}_6 - \text{dppaMe} - 2\text{Ph} - 5\text{MeO} - \text{Me}$, 50] and 698.3 [$2(\text{M}^+) - 2\text{PF}_6 - \text{dppaMe} - 2\text{Ph} - 5\text{MeO} - 2\text{Me}$, 27%].

[(OC)₃{(MeO)₃Si}Fe(μ -dppm)Pd{Ph₂PN(R)PPh₂}]_n[PF₆]_m 1h (R = (CH₂)₃Si(OEt)₃). Complex **1h** was obtained as described for **1g** from **4** (102 mg, 0.13 mmol), (Ph₂P)₂N{(CH₂)₃Si(OEt)₃} (77 mg, 0.13 mmol) and TlPF₆ (49 mg, 0.14 mmol) as a burgundy-red powder in 58% yield (143 mg) (Found: C, 52.12; H, 5.20; N, 0.82. C₆₄H₇₂F₆FeNO₉P₅PdSi requires C, 51.71; H, 4.88; N, 0.94%). $^1\text{H NMR}$ (CD_2Cl_2 , 300 MHz, 298 K): δ 0.11 (m, 2 H, SiCH₂), 0.93 (t, 9 H, $^3J_{\text{HH}} = 6$ Hz, OCH₂CH₃), 1.12 (m, 2 H, SiCH₂CH₂), 2.82 (m, 2 H, NCH₂), 3.43 (m, 15 H, Si(OMe)₃ and SiOCH₂), 3.88 (t, 2 H, PCH₂P, $^2J_{\text{PH}} = 11$ Hz) and 6.5–7.9 (m, 40 H, aromatics). Mass spectrum (FAB⁺): m/z 2142 [$2(\text{M}^+ - \text{PF}_6 - 2(\text{CH}_2)_3\text{Si}(\text{OEt})_3 - 3\text{MeO} - \text{Me}$, 13], 1284 ($\text{M}^+ - \text{PF}_6 - 2\text{CO}$, 30), 1256 ($\text{M}^+ - \text{PF}_6 - 3\text{CO}$, 100), 1207 ($\text{M}^+ - \text{PF}_6 - 2\text{CO} - \text{Ph}$, 85), 1135 ($\text{M}^+ - \text{PF}_6 - (\text{CH}_2)_3\text{Si}(\text{OEt})_3$, 15), 1079 ($\text{M}^+ - \text{PF}_6 - (\text{CH}_2)_3\text{Si}(\text{OEt})_3 - 2\text{CO}$, 25), 1002 ($\text{M}^+ - \text{PF}_6 - (\text{CH}_2)_3\text{Si}(\text{OEt})_3 - 2\text{CO} - \text{Ph}$, 34) and 997.7 [$2(\text{M}^+) - 2\text{PF}_6 - 2(\text{CH}_2)_3\text{Si}(\text{OEt})_3 - 3\text{MeO} - \text{Me}$, 14%].

[(OC)₃Fe{ μ -Si(OMe)₂(OMe)}(μ -dppa)Pd{Ph₂PCH₂C(O)-Ph}]PF₆ 2c. This complex was prepared as described for **1g** from 100 mg of **5** (0.127 mmol), 39 mg of Ph₂PCH₂C(O)Ph (0.128 mmol) and 50 mg of TlPF₆ (0.14 mmol). It was obtained as a red-brown powder in 76% yield (116 mg) (Found: C, 47.89; H, 3.83; N, 1.03. C₅₀H₄₇F₆FeNO₇P₄PdSi·CH₂Cl₂ requires C, 47.59; H, 3.84; N, 1.09%). $^1\text{H NMR}$ (CD_2Cl_2 , 300 MHz, 298 K): δ 3.45 (s, 6 H, Si(OMe)₂), 3.65 (s, 3 H, MeO→Pd), 5.10 (broad, 1 H, NH) and 6.8–7.7 (m, 35 H, aromatics).

[(OC)₃{(MeO)₃Si}Fe(μ -dppa)Pd{Ph₂PN(Me)PPh₂}]PF₆ 2g. This complex was prepared as described for **1g** from 100 mg of **5** (0.127 mmol), 52 mg of (Ph₂P)₂NMe (0.13 mmol), and 50 mg of TlPF₆ (0.14 mmol). It was obtained as a red-brown powder in 66% yield (108 mg) (Found: C, 50.57; H, 4.04; N, 2.17. C₅₅H₅₃F₆FeN₂O₆P₅PdSi requires C, 50.92; H, 4.12; N, 2.16%). $^1\text{H NMR}$ (CD_2Cl_2 , 300 MHz, 298 K): δ 2.10 (s, 3 H, NMe), 3.03 (s, 9 H, Si(OMe)₃), 4.72 (broad, 1 H, NH) and 6.7–7.9 (m, 40 H, aromatics).

[(OC)₃Fe{ μ -Si(OMe)₂(OMe)}(μ -dppm)Pt{Ph₂PC₆H₄(*o*-OMe)}]PF₆ 3a. This complex was prepared in a similar manner to **1a** from 200 mg of **6** (0.228 mmol), 67 mg of Ph₂P{C₆H₄(*o*-OMe)} (0.23 mmol), and 87 mg of TlPF₆ (0.25 mmol). It was obtained as a yellow-brown microcrystals in 79% yield (230 mg) (Found: C, 46.00; H, 3.75. C₅₀H₄₈F₆FeO₇P₄PtSi·0.5CH₂Cl₂ requires C, 45.94; H, 3.74%). $^1\text{H NMR}$ (CD_2Cl_2 , 300 MHz, 298 K): δ 2.88 (s, 3 H, MeO→Pt), 3.47 (s, 3 H, OMe phosphine), 3.73 (s, 6 H, Si(OMe)₂), 3.96 (t, 2 H, PCH₂P, $J_{\text{PH}} = 10$ Hz) and 6.8–7.7 (m, 34 H, aromatics).

[(OC)₃Fe{ μ -Si(OMe)₂(OMe)}(μ -dppa)PdCl] 5. The hydrido complex [FeH{Si(OMe)₃}(CO)₃(dppa-P)] was formed *in situ* by photochemical oxidative addition of HSi(OMe)₃ (1.15 ml, 9 mmol) to [Fe(CO)₅] (0.4 ml, 3 mmol) in hexane (100 ml) followed by addition of 0.646 g (Ph₂P)₂NH (dppa, 2.8 mmol). This procedure is similar to that previously described for [FeH{Si(OMe)₃}(CO)₃(dppm-P)].^{4b} Addition of NEt₃ (0.4 ml, 0.28 mmol) caused precipitation of [HNEt₃][Fe{Si(OMe)₃}(CO)₃(dppa-P)]. The reaction mixture was kept at -20°C for 2 d. The solvent was then decanted and the residue dried under reduced pressure and redissolved in dichloromethane.

The solution was cooled to $-30\text{ }^{\circ}\text{C}$ and $[\text{PdCl}_2(\text{COD})]$ (0.77 g, 2.7 mmol) added. After the solution had been stirred at room temperature for 1 h it was filtered through a 3 cm pad of silica and Celite. The solvent was then removed under reduced pressure and **5** was obtained as a yellow powder in 62% yield based on Pd (1.32 g) (Found: C, 45.48; H, 4.07; N, 1.80. $\text{C}_{30}\text{H}_{30}\text{ClFeNO}_6\text{P}_2\text{PdSi}$ requires C, 45.71; H, 3.84; N, 1.78%). $\nu(\text{CO})$ (hexane) 2002s, 1955s and 1918w cm^{-1} . ^1H NMR (CD_2Cl_2 , 300 MHz, 298 K): δ 3.70 (br, 9 H, $\text{Si}(\text{OMe})_3$) and 4.5 (br, NH). $^{31}\text{P}\{-^1\text{H}\}$ NMR (CD_2Cl_2 , 121 MHz, 298 K): δ 85.8 (d, $^{2+3}J_{\text{PP}} = 51$, P(Pd)) and 100.8 (d, $^{2+3}J_{\text{PP}} = 51$ Hz, P(Fe)).

[(OC)₃Fe{ μ -Si(OMe)₂(OMe)}(μ -dppm)Pd(PPh₃)]PF₆ 7a.

This complex was prepared in a similar manner to **1a** from 150 mg of **4** (0.19 mmol), 52 mg of PPh₃ (0.20 mmol), and 76 mg of TIPF₆ (0.22 mmol). It was obtained as a red powder in 80% yield (175 mg) (Found: C, 50.31; H, 4.08. $\text{C}_{49}\text{H}_{46}\text{F}_6\text{FeO}_6\text{P}_4\text{PdSi}$ requires C, 50.77; H, 4.00%). ^1H NMR (CD_2Cl_2 , 300 MHz, 298 K): δ 3.47 (broad, 9 H, $\text{Si}(\text{OMe})_3$), 4.19 (t, 2 H, PCH_2P , $^2J_{\text{PH}} = 10.5$ Hz) and 6.8–7.9 (m, 35 H, aromatics).

[(OC)₃Fe{ μ -Si(OMe)₂(OMe)}(μ -dppm)Pd(AsPh₃)]PF₆ 7b.

This complex was prepared as described for **1a** from 150 mg of **4** (0.19 mmol), 61 mg of AsPh₃ (0.20 mmol), and 76 mg of TIPF₆ (0.22 mmol). It was obtained as a red powder in 74% yield (170 mg) (Found: C, 48.65; H, 4.14. $\text{C}_{49}\text{H}_{46}\text{AsF}_6\text{FeO}_6\text{P}_4\text{PdSi}$ requires C, 48.92; H, 3.85%). ^1H NMR (CD_2Cl_2 , 300 MHz, 298 K): δ 2.89 (s, 3 H, MeO→Pd), 3.77 (s, 6 H, $\text{Si}(\text{OMe})_2$), 4.13 (t, 2 H, PCH_2P , $^2J_{\text{PH}} = 10.5$ Hz) and 7.0–7.9 (m, 35 H, aromatics).

[(OC)₃Fe{ μ -Si(OMe)₂(OMe)}(μ -dppm)Pt(PPh₃)]PF₆ 8a. This complex was prepared as described for **1a** from 200 mg of **6** (0.228 mmol), 60 mg of PPh₃ (0.23 mmol), and 84 mg of TIPF₆ (0.24 mmol). It was obtained as a yellow powder in 71% yield (200 mg) (Found: C, 47.42; H, 3.76. $\text{C}_{49}\text{H}_{46}\text{F}_6\text{FeO}_6\text{P}_4\text{PtSi}$ requires C, 47.17; H, 3.71%). ^1H NMR (CD_2Cl_2 , 300 MHz, 298 K): δ 2.88 (s, 3 H, MeO→Pt), 3.79 (s, 6 H, $\text{Si}(\text{OMe})_2$), 3.94 (t, 2 H, PCH_2P , $^2J_{\text{PH}} = 10.5$ Hz) and 6.8–7.9 (m, 35 H, aromatics).

[(OC)₃Fe{ μ -Si(OMe)₂(OMe)}(μ -dppm)Pt(AsPh₃)]PF₆ 8b.

This complex was prepared as described for **1a** from 200 mg of **6** (0.228 mmol), 70 mg of AsPh₃ (0.23 mmol), and 84 mg of TIPF₆ (0.24 mmol). It was obtained as a red powder in 77% yield (225 mg) (Found: C, 44.07; H, 3.19. $\text{C}_{49}\text{H}_{46}\text{AsF}_6\text{FeO}_6\text{P}_4\text{PtSi}$ requires C, 43.62; H, 3.51%). ^1H NMR (CD_2Cl_2 , 300 MHz, 298 K): δ 3.13 (s, 3 H, MeO→Pt), 3.81 (s, 6 H, $\text{Si}(\text{OMe})_2$), 3.95 (dd, 2 H, PCH_2P , $^2J_{\text{PH}} = 9.8$ and 11.2 Hz) and 7.0–7.8 (m, 35 H, aromatics).

[PdCl(dppm-*P,P'*)]{Ph₂P{C₆H₄(*o*-OMe)}]PF₆ g. A mixture of 150 mg of $[\text{PdCl}_2(\text{dppm-}P,P')]$ (0.267 mmol) and 78 mg of $\text{Ph}_2\text{P}\{\text{C}_6\text{H}_4(\textit{o}\text{-OMe})\}$ (0.267 mmol) in CH_2Cl_2 (20 ml) was cooled to $-40\text{ }^{\circ}\text{C}$ and treated with 95 mg of TIPF₆ (0.27 mmol). The reaction mixture was allowed to warm to room temperature, stirred for 1 h at this temperature, filtered over a Celite pad and concentrated to ca. 3 ml. Addition of Et₂O afforded a yellow-orange precipitate. The solvent was removed via a canula and the residue washed with pentane (2 × 10 ml) and dried *in vacuo*. Complex **g** was obtained as a yellow-orange powder in 62% yield (160 mg) (Found: C, 54.96; H, 3.94. $\text{C}_{44}\text{H}_{39}\text{ClF}_6\text{FeOP}_4\text{Pd}$ requires C, 54.85; H, 4.08%). ^1H NMR (CD_2Cl_2 , 300 MHz, 298 K): δ 3.74 (s, 3 H, OMe), 3.79 (t, 2 H, PCH_2P , $^2J_{\text{PH}} = 11$ Hz) and 6.8–7.8 (m, 34 H, aromatics). $^{31}\text{P}\{-^1\text{H}\}$ NMR (CD_2Cl_2 , 298 K): δ -143.6 (sept, PF₆, $^1J_{\text{PF}} = 709$), -48.2 (dd, dppm, P *trans* P, $^2J_{\text{PP}trans} = 484$, $^2J_{\text{PP}} = 81$), -38.3 (d, dppm, P *trans* Cl, $^2J_{\text{PP}} = 81$) and 16.04 (d, $\text{Ph}_2\text{PC}_6\text{H}_4(\textit{o}\text{-OMe})$, $^2J_{\text{PP}trans} = 484$ Hz).

Collection of the X-ray data and structure determination for complexes 9 and 10

Single crystals suitable for X-ray diffraction were obtained from CH_2Cl_2 -toluene-hexane. Data were collected on a Nonius MACH-3 diffractometer using Mo-K α graphite monochromated radiation ($\lambda = 0.7107\text{ \AA}$), θ - 2θ scans. The structures were solved using direct methods and refined against $|F|$. Absorption corrections were computed from the ψ scans of four reflections. For all computations; the Nonius MoLEN package²⁴ was used.

Crystal data for complex 9. Yellow crystals, data collected at 293 K (crystal dimensions $0.35 \times 0.40 \times 0.40$ mm): $\text{C}_{44}\text{H}_{39}\text{ClF}_6\text{OP}_4\text{Pd}\cdot\text{C}_7\text{H}_8$, $M = 1055.7$, monoclinic, space group $P2_1/c$, $a = 11.500(3)$, $b = 20.814(6)$, $c = 21.055(6)\text{ \AA}$, $\beta = 97.92(2)^\circ$, $V = 4991.4\text{ \AA}^3$, $Z = 4$, $D_c = 1.405\text{ g cm}^{-3}$, $\mu(\text{Mo-K}\alpha) = 6.028\text{ cm}^{-1}$. A total of 15846 reflections were collected, $2 < \theta < 30^\circ$, 8137 having $I > 3\sigma(I)$. Absorption factors 0.98/1.00, 542 parameters. Final $R(F) = 0.051$, $R_w(F) = 0.080$, Goodness of fit = 1.528, maximum residual electron density 1.26 e \AA^{-3} . All non-hydrogen atoms were refined anisotropically with the exception of the toluene C atoms. The hydrogen atoms were introduced as fixed contributors ($d_{\text{C-H}} = 0.95\text{ \AA}$, $B_{\text{H}} = 1.3B_{\text{equiv}}(\text{C})\text{ \AA}^2$); toluene protons were omitted.

Crystal data for complex 10. Red crystals, data collected at 173 K (crystal dimensions $0.60 \times 0.40 \times 0.20$ mm): $\text{C}_{51}\text{H}_{44}\text{OP}_4\text{Cl}_2\text{Pd}_2\cdot 3\text{CH}_2\text{Cl}_2\cdot\text{H}_2\text{O}$, $M = 1353.3$, tetragonal, space group $P4_1$, $a = 21.171(6)$, $c = 14.309(4)\text{ \AA}$, $V = 6413.4\text{ \AA}^3$, $Z = 4$, $D_c = 1.402\text{ g cm}^{-3}$, $\mu(\text{Mo-K}\alpha) = 10.228\text{ cm}^{-1}$. A total of 9185 reflections were collected, $2 < \theta < 29^\circ$, 7135 having $I > 3\sigma(I)$. Absorption factors 0.89/1.00, 639 parameters. Final $R(F) = 0.036$, $R_w(F) = 0.053$, Goodness of fit = 1.167, maximum residual electron density 0.12 e \AA^{-3} . All non-hydrogen atoms were refined anisotropically. The hydrogen atoms were introduced as fixed contributors ($d_{\text{C-H}} = 0.95\text{ \AA}$, $B_{\text{H}} = 1.3B_{\text{equiv}}(\text{C})\text{ \AA}^2$); water protons were omitted.

CCDC reference number 186/1457.

See <http://www.rsc.org/suppdata/dt/1999/2159/> for crystallographic files in .cif format.

Acknowledgements

We are grateful to T. Faure for preliminary studies on complex **1b** and thank the SOCRATES Mobility Scheme between RWTH Aachen, Germany and Université Louis Pasteur, Strasbourg, France for a grant to T. W. We are grateful to the Centre National de la Recherche Scientifique for financial support and to Johnson Matthey plc for a generous loan of PdCl_2 .

References

- See for example: K. M. Mackay and B. K. Nicholson, in *Comprehensive Organometallic Chemistry*, eds. G. Wilkinson, F. G. A. Stone and E. W. Abel, Pergamon, Oxford, 1982, ch. 43; I. Ojima, in *The Chemistry Organic Silicon Compounds*, eds. S. Patai and Z. Rappoport, Wiley, Chichester, 1989, p. 1479; T. D. Tilley, in *The Silicon-Heteroatom Bond*, eds. S. Patai and Z. Rappoport, Wiley-Interscience, New York, 1991, pp. 245–309; C. Zybille, H. Handwecker and H. Friedrich, *Adv. Organomet. Chem.*, 1994, **36**, 229; P. Braunstein and M. Knorr, *J. Organomet. Chem.*, 1995, **500**, 21.
- See for recent reviews: D. F. Shriver, H. D. Kaesz and R. D. Adams, in *The Chemistry of Metal Cluster Complexes*, VCH, Weinheim, 1990; G. Schmid, in *Aspects of Homogeneous Catalysis*, ed. R. Ugo, Kluwer, Dordrecht, 1990, vol. 7, pp. 1–36; P. Braunstein, *New J. Chem.*, 1988, **12**, 307; P. Braunstein and J. Rosé, in *Stereochemistry of Organometallic and Inorganic Compounds*, ed. I. Bernal, Elsevier, Amsterdam, 1989, vol. 3, ch. 1, pp. 3–138; P. Braunstein, in *Perspectives in Coordination Chemistry*, eds. A. F. Williams,

- C. Floriani and A. E. Merbach, VCH, Weinheim, 1992, pp. 67–107; P. Braunstein and J. Rosé, in *Comprehensive Organometallic Chemistry II*, Elsevier, New York, 1995, vol. 10, pp. 351–385; *Heterometallic Clusters for Heterogeneous Catalysis*, eds. R. D. Adams and F. A. Cotton, Wiley-VCH, New York, 1998, pp. 443–508; *Metal Clusters in Chemistry*, eds. P. Braunstein, L. A. Oro and P. R. Raithby, Wiley-VCH, Weinheim, 1999, in the press.
- 3 (a) P. Braunstein, M. Knorr and C. Stern, *Coord. Chem. Rev.*, 1998, **178–180**, 903 and refs. therein. (b) P. Braunstein, M. Knorr, A. Tiripicchio and M. Tiripicchio Camellini, *Angew. Chem., Int. Ed. Engl.*, 1989, **28**, 1361; (c) P. Braunstein, M. Knorr, H. Piana and U. Schubert, *Organometallics*, 1991, **10**, 828.
- 4 (a) P. Braunstein, M. Knorr, E. Villarroya and J. Fischer, *New J. Chem.*, 1989, **14**, 583; (b) P. Braunstein, M. Knorr, U. Schubert, M. Lanfranchi and A. Tiripicchio, *J. Chem. Soc., Dalton Trans.*, 1991, 1507; (c) P. Braunstein, M. Knorr, E. Villarroya, A. DeCian and J. Fischer, *Organometallics*, 1991, **10**, 3714; (d) F. Balegroune, P. Braunstein, L. Douce, Y. Dusausoy, D. Grandjean, M. Knorr and M. Strampfer, *J. Cluster Sci.*, 1992, **3**, 275; (e) P. Braunstein, L. Douce, M. Knorr, M. Strampfer, M. Lanfranchi and A. Tiripicchio, *J. Chem. Soc., Dalton Trans.*, 1992, 331; (f) G. Reinhard, B. Hirle, U. Schubert, M. Knorr, P. Braunstein, A. DeCian and J. Fischer, *Inorg. Chem.*, 1993, **32**, 1656; (g) P. Braunstein, M. Knorr, M. Strampfer, A. DeCian and J. Fischer, *J. Chem. Soc., Dalton Trans.*, 1994, 117; (h) P. Braunstein, J. Durand, M. Knorr, X. Morise, R. Pugin, G. Kickelbick and U. Schubert, in preparation.
- 5 (a) P. Braunstein, M. Knorr and T. Stährfeldt, *J. Chem. Soc., Chem. Commun.*, 1994, 1913; (b) P. Braunstein, T. Faure, M. Knorr, T. Stährfeldt, A. DeCian and J. Fischer, *Gazz. Chim. Ital.*, 1995, **125**, 35; (c) M. Knorr, P. Braunstein, A. DeCian and J. Fischer, *Organometallics*, 1995, **14**, 1302; (d) M. Knorr, C. Strohmam and P. Braunstein, *Organometallics*, 1996, **15**, 5653; (e) P. Braunstein, M. Knorr, J. Cossy, C. Strohmam and P. Vogel, unpublished results.
- 6 P. Braunstein and X. Morise, *Organometallics*, 1998, **17**, 540.
- 7 L. S. Benner and A. L. Balch, *J. Am. Chem. Soc.*, 1978, **100**, 6099.
- 8 P. Braunstein, T. Faure, M. Knorr, F. Balegroune and D. Grandjean, *J. Organomet. Chem.*, 1993, **462**, 271.
- 9 (a) K. R. Dunbar and J.-S. Sun, *J. Chem. Soc., Chem. Commun.*, 1994, 2387 and refs. therein; (b) J.-S. Sun, C. E. Uzelmeier, D. L. Ward and K. R. Dunbar, *Polyhedron*, 1998, **17**, 2049.
- 10 S.-E. Bouaoud, P. Braunstein, D. Grandjean, D. Matt and D. Nobel, *Inorg. Chem.*, 1986, **25**, 3765; P. Braunstein, D. Matt, D. Nobel, F. Balegroune, S.-E. Bouaoud, D. Grandjean and J. Fischer, *J. Chem. Soc., Dalton Trans.*, 1998, 353.
- 11 J. Andrieu, P. Braunstein and A. D. Burrows, *J. Chem. Res. (S)*, 1993, 380.
- 12 P. E. Garrou, *Chem. Rev.*, 1981, **81**, 229.
- 13 P. Braunstein and X. Morise, unpublished results.
- 14 C. K. Johnson, ORTEP, Report ORNL-5138, Oak Ridge National Laboratory, Oak Ridge, TN, 1976.
- 15 C. P. Kubiak and R. Eisenberg, *J. Am. Chem. Soc.*, 1977, **99**, 6129.
- 16 M. L. Kullberg and C. P. Kubiak, *Organometallics*, 1984, **3**, 632.
- 17 A. L. Balch, L. S. Benner and M. A. Olmstead, *Inorg. Chem.*, 1979, **18**, 2996.
- 18 D. J. Wink, B. T. Creagan and S. Lee, *Inorg. Chim. Acta*, 1991, **180**, 183.
- 19 S. R. Klopfenstein, C. Kluwe, K. Kirschbaum and J. A. Davies, *Can. J. Chem.*, 1996, **74**, 2331.
- 20 C.-L. Lee, Y.-P. Yang, S. J. Rettig, B. R. James, D. A. Nelson and M. A. Lilga, *Organometallics*, 1986, **5**, 2220.
- 21 F. T. Wang, J. Najdzionek, K. L. Leneker, H. Wassermen and D. M. Braitsch, *Synth. React. Inorg. Metal-Org. Chem.*, 1978, **8**, 119.
- 22 I. Bachert, P. Braunstein and R. Hasselbring, *New J. Chem.*, 1996, **20**, 993.
- 23 M. Habib, H. Trujillo, C. A. Alexander and B. N. Storhoff, *Inorg. Chem.*, 1985, **24**, 2344.
- 24 C. K. Fair, MOLEN, An Interactive Intelligent System for Crystal Structure Analysis, Nonius, Delft, 1990.

Paper 9/00390H